1 **Identifying rhodopsin-containing cells using TIRF microscopy**

2 J.L. Keffer[1], C.R. Sabanayagam[2], M.E. Lee[3,†], E.F. DeLong[4], M.W. Hahn[5], J.A.
3 Maresca[1,*]
4 [1]Dept. of Civil and Environmental Engineering, University of Delaware, Newark DE
5 19716 USA
6 [2]Delaware Biotechnology Institute, Newark DE 19716 USA
7 [3]Dept. of Biological Engineering, Massachusetts Institute of Technology, Cambridge MA
8 02139 USA
9 [4]Dept. of Civil and Environmental Engineering, Massachusetts Institute of Technology,
10 Cambridge MA 02139 USA
11 [5]Research Institute for Limnology, University of Innsbruck, Mondsee Austria
12
13 *To whom correspondence should be addressed: 301 DuPont Hall, Newark, DE 19716
14 USA. Telephone: (302) 831-4391, Fax (302) 831-3640. Email jmaresca@udel.edu
15
16 **Running title: Visualizing rhodopsins *in vivo***
17
18
19
20 [†]Current address: Department of Bioengineering, University of California, Berkeley,
21 Berkeley, CA 94720 USA
22

Summary

Sunlight is captured and converted to chemical energy in illuminated environments. Although (bacterio)chlorophyll-based photosystems have been characterized in detail, retinal-based photosystems, rhodopsins, have only recently been identified as important mediators of light energy capture and conversion. Recent estimates suggest that up to 70% of cells in some environments harbor rhodopsins. However, because rhodopsin autofluorescence is low – comparable to that of carotenoids, and significantly less than that of (bacterio)chlorophylls – these estimates are based on metagenomic sequence data, not direct observation. We report here the use of ultrasensitive total internal reflection fluorescence (TIRF) microscopy to distinguish between unpigmented, carotenoid-producing, and rhodopsin-expressing bacteria. *E. coli* were engineered to produce lycopene, β-carotene, or retinal. A gene encoding an uncharacterized rhodopsin, actinorhodopsin, was cloned into retinal-producing *E. coli*. The production of correctly folded and membrane-incorporated actinorhodopsin was confirmed via development of pink color in *E. coli* and SDS-PAGE. Cells expressing carotenoids or actinorhodopsin were imaged by TIRF microscopy. The 561 nm excitation laser specifically illuminated rhodopsin-containing cells, allowing them to be differentiated from unpigmented and carotenoid-containing cells. Furthermore, water samples collected from the Delaware River were shown to contain rhodopsin-containing organisms by PCR and were examined by TIRF microscopy. Individual microorganisms were identified that fluoresced under illumination from the 561 nm laser. These results verify the sensitivity of the TIRF microscopy method for visualizing and distinguishing between different molecules with low autofluorescence, making it useful for analyzing natural samples.

46

47 **Introduction**

48 Sunlight powers most carbon fixation, and the organic carbon produced via
49 photosynthesis is the base of ecological metabolic interactions (1). Photoheterotrophs use
50 sunlight for energy, but consume organic carbon, rather than produce it. The anoxygenic
51 photoheterotrophs that harvest light with bacteriochlorophyll (BChl)-dependent
52 photosystems have been characterized in detail, and their contributions to the global
53 carbon cycle are well-documented (2). Recent work suggests that a surprisingly large
54 number of photoheterotrophic microbes may capture light energy with a retinal-based,
55 single-polypeptide photosystem, rhodopsin (3), which uses light energy to generate an
56 electrochemical gradient across the cytoplasmic membrane that can be used for motility
57 (4), solute transport, or ATP synthesis (5, 6). In order to determine how light energy can
58 be used by different organisms and to accurately quantify the number of organisms that
59 use light, we must be able to identify not only chlorophyll (Chl)-containing organisms,
60 but also rhodopsin-containing cells in environmental samples.

61

62 Rhodopsins are light-sensing membrane proteins with a retinal cofactor, which undergoes
63 a conformational change in response to absorption of a photon (7). This conformational
64 change drives either transfer of information, via protein-protein interactions and the
65 regulation of the expression of other genes in response to light (8), or by transport of an
66 ion across the membrane (7). Photosensory rhodopsins, which sense light and transmit a
67 signal to other proteins, are the basis for vision in vertebrates and many invertebrates, and
68 are found in plants and fungi as well as a variety of prokaryotic species (7). Most

characterized microbial rhodopsins transport protons in response to light, and are thus used to maintain the proton motive force (7), though some pump Na^+ or Cl^- (9–11). Proton-pumping microbial rhodopsins include the proteorhodopsins of marine bacteria (12), bacteriorhodopsins of archaea (13), the xanthorhodopsins of *Salinibacter ruber* (6), and the recently identified actinorhodopsins (14). Actinorhodopsins are predicted to be light-activated proton pumps, and are found in freshwater Actinobacteria (14–16). Proton-pumping rhodopsins are hypothesized to supplement the cellular energy budget under low-nutrient conditions (3, 17–19), and heterologous expression experiments have demonstrated elevated ATP production in starved, proteorhodopsin-expressing *E. coli* cells exposed to light (20).

Given the diversity of function, it is perhaps unsurprising that rhodopsins are widespread in illuminated environments. However, detection of rhodopsins in environmental samples has been hampered by the low fluorescent yield of rhodopsin and its light-absorbing cofactor retinal. Neither can be detected using the fluorescence-based assays such as those developed for *in vivo* quantification of Chl *a* or BChl *a* in natural samples (21–23). Instead, rhodopsin abundance has been calculated based on metagenomic sequence data (3, 12, 24, 25), amplicon sequencing (15, 26, 27), quantitative polymerase chain reaction (QPCR) (27, 28) or cultivation (15, 29–31). These estimates show that in some marine environments, up to 70% of the cells may host a rhodopsin (3), while up to 30% are Chl *a*-containing cyanobacteria (32, 33), and an additional 1-30% contain BChl *a* (34). In non-marine aquatic environments, 35-62% of genomes within metagenomic assemblies harbor a rhodopsin (14), while analysis of freshwater bacterioplankton metagenomic

assemblies and single amplified genomes from the same locations suggested the presence of a rhodopsin in 37-56% and 8-20% of the samples, respectively (35). These studies have demonstrated that rhodopsins are both more abundant and more diverse than previously suspected (10, 36–38). However, metagenomic and metatranscriptomic data cannot demonstrate that a rhodopsin is functional, nor can they consistently identify the organism that hosts the rhodopsin. To confirm the hypothesis that in some environments, the majority of prokaryotes respond to sunlight, it must be possible to detect and quantify rhodopsin-producing cells in natural samples.

Rhodopsin fluorescence, though faint (39), has a characteristic absorption peak in the 480-560 nm range and fluoresces in the 600-900 nm range (40), with a very low fluorescent yield, approximately 10^{-5} to 10^{-4} (40–42). Because of the low fluorescent yield, detecting and monitoring rhodopsin fluorescence has been difficult without bulk measurement of large numbers of cells or instrumentation that includes signal amplification for single-cell analysis (42). Here we report a method that uses through-the-objective total internal reflection fluorescence (TIRF) microscopy (43) to differentiate between rhodopsin-containing and pigmented cells. TIRF microscopy relies on the total internal reflection phenomenon that takes place when light encounters an interface between two different refractive indexes (i.e., the coverglass and liquid media). The evanescent field extends only a few hundred nanometers above the coverglass but is able to excite fluorescent molecules at the coverglass-cell interface. Because a relatively small excitation volume is created with TIRF microscopy, background contributions from Raman scattering from the liquid media are greatly reduced, enabling the detection of

Applied and Environmental Microbiology

115 weakly fluorescent surface-bound molecules. This method is sensitive enough to detect
116 fluorescence due to rhodopsins and carotenoid pigments, precursors to the retinal cofactor
117 in rhodopsins, and can differentiate between them with the appropriate excitation
118 wavelength. Using TIRF microscopy, direct detection of rhodopsin-containing cells in
119 natural samples becomes possible.
120
121 **Materials and Methods**
122 *Strains and growth conditions.* Actinobacterial strain *Rhodoluna lacicola* strain MWH-
123 Ta8 (15, 16, 29) was grown in 3 g L^{-1} NSY medium (44) at room temperature with gentle
124 shaking. *E. coli* strain epi300 (Epicentre Biotechnology, catalog number EC300105) was
125 used for carotenoid biosynthesis and actinorhodopsin expression. These cells were grown
126 in Luria-Bertani medium supplemented with 100 mg L^{-1} ampicillin, and/or 34 mg L^{-1}
127 chloramphenicol, as appropriate, for plasmid propagation, and with antibiotics and 0.02-
128 0.2% L-arabinose for carotenoid expression.
129
130 *Carotenoid-synthesizing* E. coli *strains.* Plasmids with genes encoding the synthesis of
131 lycopene, β-carotene, and retinal were constructed by PCR amplification of the relevant
132 genes from marine alphaproteobacterial fosmid HF10_19P19 (20) (see Table 1 for primer
133 sequences and Figure 1 for amplicons). The plasmid pLY02, encoding production of
134 lycopene (Fig. 1), was constructed by amplification of the region encoding *crtE*
135 (geranylgeranyldiphosphate synthase), *crtI* (phytoene dehydrogenase), and *crtB*
136 (phytoene synthase) from HF10_19P19, using primers 19P19_F1 and 19P19_R1, and
137 insertion into the TA cloning site of the pBAD-TOPO vector (Life Technologies K4300-

40). The plasmid pBC01, encoding β-carotene biosynthesis, was constructed by amplifying a slightly larger region that also included the lycopene cyclase, *crtY*, using primers 19P19_F1 and 19P19_R2 (see Table 1 and Fig. 1). The reverse primer for this reaction includes an endogenous XbaI site. To make plasmid pRET04, encoding retinal biosynthesis, the region immediately downstream of the region included in plasmid pBC01 was amplified from HF10_19P19 using primers 19P19_F3 (the reverse/complement of primer 19P19_R2) and 19P19_R3 (Fig. 1). This region covers the *blh* gene, encoding a β-carotene cleavage dioxygenase, which produces retinal from β-carotene. The PCR product was digested with XbaI, and plasmid pBC01 was digested with XbaI and the blunt cutter PmeI. Both the linearized plasmid and digested PCR product were gel-purified and ligated, and the ligation product was transformed into *E. coli*.

Cloning, expression, and partial purification of actinorhodopsin. The gene *actR* (NCBI accession number FJ545221), encoding actinorhodopsin, was amplified from DNA extracted from *Rhodoluna lacicola* strain MWH-Ta8 using primers F-apa-ta8 and R-ta8-bam (Table 1). PCR reactions were performed utilizing Phusion DNA Polymerase (Thermo Scientific). The amplification steps were: initial denaturation at 98 ^{o}C for 30 sec., then 35 cycles of 98 ^{o}C for 10 sec., 50 ^{o}C for 30 sec., 72 ^{o}C for 24 sec., then a final elongation step of 72 ^{o}C for 10 min. The ~800 bp amplification product was inserted into plasmid pMCL200 (45) at the ApaI/BamHI restriction sites to produce plasmid pTAR, and the insert was sequenced. Plasmid pTAR was transformed into *E. coli* epi300/pRET04 to create a strain co-expressing actinorhodopsin and its cofactor, retinal.

An empty-vector control strain was created by transforming pMCL200 into *E. coli* epi300/pRET04. Membranes from *E. coli* harboring pRET04 along with either pTAR or pMCL200 were partially purified by incubating the cells with an osmotic lysis buffer containing lysozyme (0.075 M Tris pH 8.0, 2.0 mM $MgSO_4$, 0.4 M sucrose, 10 mg mL^{-1} lysozyme) for 1 hour at 37 ^{o}C with shaking, followed by centrifugation at 4500 × *g* for 20 min. at 4 ^{o}C. The supernatant was removed and the cell pellet resuspended in a high salt buffer (50 mM Tris pH 7.6, 10 mM $MgSO_4$, 0.8 M NaCl) and briefly sonicated (46). After broken cells were centrifuged at 25000 × *g* for 30 min. at 4 ^{o}C, a dull-colored cell debris pellet was obtained, covered by a brightly-colored membrane film. The membrane film was removed and resuspended in 3% beta-octylglucopyranoside (Amresco) in 10 mM HEPES, pH 7.1 by vortexing overnight at 4 ^{o}C in the dark. The detergent-solubilized membrane was centrifuged at 11000 × *g* for 10 min. at 4 ^{o}C to remove insoluble material. Absorption spectra from 250 – 900 nm were recorded using a Thermo Scientific BioMate 3S UV-Visible Spectrophotometer. The membrane fraction of cells harboring pRET04 and pMCL200 was used as the blank. Membrane preparations to be analyzed by sodium dodecyl sulfate-polyacrylamide gel electrophoresis (SDS-PAGE) were incubated 1:1 in 2X loading buffer (250 mM Tris, 2% SDS, 30% glycerol, 10% 2-mercaptoethanol, 0.002% bromophenol blue) for 1 hour at room temperature. Samples were loaded on a 10% Tris-buffered polyacrylamide resolving gel, topped with a 5% polyacrylamide stacking gel and electrophoresed according to the method of Laemmli (47). The molecular weight standard was PageRuler Prestained Protein Ladder 10-170 kDa (Thermo Scientific).The gel was washed with DI water, fixed with 10:25:65 glacial acetic acid:methanol:water for 15 min., and stained with LabSafe GEL Blue (G-Biosciences).

184

185 *HPLC analysis*. For pigment analysis by high-performance liquid chromatography
186 (HPLC), *E. coli* cells containing plasmids pLY02, pBC01, and pRET04 were grown in
187 LB with 50 mg L^{-1} ampicillin overnight at 30 ^{o}C with shaking in the presence of either
188 0.2% glucose or 0.02% arabinose. Cells were harvested by centrifugation and washed
189 once with TES buffer (200 mM Tris pH 8.0, 20 mM EDTA, 200 mM NaCl). Pigments
190 were extracted from cells by sonication in acetone:methanol (7:2 v/v). Cell debris was
191 removed by centrifugation, and supernatants were filtered through 0.2 µm
192 polytetrafluoroethylene syringe filters (Thermo Scientific) prior to injection into the
193 HPLC. The HPLC system was a Shimadzu Prominence system with solvent degasser
194 (DGU-20A5), quaternary pump (LC-20AT), and 996-element diode array detector (SPD-
195 M20A) fitted with a Supelco Ascentis reverse-phase C18 column (100 × 3 mm, 3 µm
196 beads; Sigma-Aldrich catalog number 581308-U). Solvent A was 62.5% water, 21%
197 methanol, and 16.5% acetonitrile, buffered with 10 mM ammonium acetate, and solvent
198 B was 50% methanol, 30% ethyl acetate and 20% acetonitrile by volume (48). The
199 gradient was as follows (min., %B): (0, 20), (5, 70), (12,100), (25,100). The column was
200 kept at a constant temperature of 35 °C.

201

202 *Delaware River water collection, genomic DNA isolation and rhodopsin PCR.* Twenty
203 liters of Delaware River water was collected October 28, 2014 from Battery Park in New
204 Castle, Delaware (39^{o}39′27.1″N, 75^{o}33′48.2″W). The water was filtered through 1 mm
205 nylon into a washed and rinsed Nalgene bottle. At the time of collection, the water
206 temperature was 18 ^{o}C, and the salinity was ~11 ppt. Genomic DNA was extracted from

100 mL of water that was filtered through a 1.0 µm cellulose nitrate filter (Whatman) and onto a 0.22 µm MoBio filter in triplicate. Genomic DNA was extracted using the MoBio Rapid Water kit (MoBio, catalog # 14810-50-NF) per the manufacturer's instructions. The genomic DNA was screened for the presence of rhodopsin genes using degenerate primers for actinorhodopsin (15) and proteorhodopsin (28) (Table 1 and Table SI-1). A positive result was obtained using the SARPR_125F and SARPR_203R primer pair with Taq polymerase (Sigma-Aldrich, catalog # D4545-250UN) and thermocycling conditions of 94 ^{o}C for 3 min., then 40 cycles of 94 ^{o}C for 1 min., 54 ^{o}C for 1 min., 72 ^{o}C for 1 min., then a final elongation step of 72 ^{o}C for 5 min. The PCR products were cloned into the TOPO TA sequencing vector (Life Technologies, catalog # K4575-01) and sequenced by the University of Delaware Sequencing and Genotyping Center. Sequences were trimmed of the vector sequence and aligned using the SeaView and Clustal programs. Nucleotide sequences were deposited in GenBank with accession numbers KP343692-KP343697.

Sample preparation for live-cell TIRF microscopy. *E. coli* with plasmid(s) pLY02, pBC01, pRET04, pRET04/pMCL200, pRET04/pTAR, or pTAR were grown in LB with appropriate antibiotics overnight at 30 ^{o}C with shaking. Expression of pigments and rhodopsin was induced with arabinose (0.2 g L^{-1}). One milliliter of cell culture was harvested by centrifugation at 3500 x *g* for 5 min. The cells were washed with DI water twice, and resuspended in 75 µL of water. Fifty microliters of cells were added to each chamber of a LabTekII chambered #1.5 German coverglass system (Nunc 155409) that had been previously treated with 100 µL of 0.5% (w/v) gelatin (Sigma G6144) with

Applied and Environmental Microbiology

229 0.01% (w/v) chromium ammonium sulfate, then dried under vacuum (49). After 10
230 minutes, unattached cells were removed, and 100 µL LB media was added to the wells.
231
232 *Sample preparation for fixed-cell TIRF microscopy.* Fisherbrand coverglasses (22 × 22
233 #1.0) were cleaned with several washes of DI water, followed by sonication for 15
234 minutes in fresh DI water (2X). The coverglasses were then placed in 0.1 N HCl for 1
235 hour with shaking, washed 3X with DI water, and soaked in 95% ethanol for 1 hour with
236 shaking. The coverglasses were rinsed 2X with DI water and stored in 95% ethanol until
237 use. Washed coverslips were removed from ethanol, air-dried, and sterilized with 15 min.
238 exposure to UV light. The coverslips were then dipped in 0.5% (w/v) gelatin (Sigma
239 G6144) with 0.01% (w/v) chromium ammonium sulfate, and air-dried overnight at an
240 angle. *E. coli* expressing retinal-containing actinorhodopsin was fixed with 4%
241 paraformaldehyde for 15 minutes at 4 ^{o}C and visualized by TIRF microscopy to confirm
242 that fixing the cells did not affect the rhodopsin fluorescence (data not shown). Twenty
243 milliliters of Delaware River water was filtered through a 1.0 µm cellulose nitrate filter
244 (Whatman) and fixed with paraformaldehyde (Electron Microscopy Sciences; 4% final
245 concentration) overnight at 4 ^{o}C. The entire 20 mL volume was concentrated to ~3 mL on
246 a 25 mm 0.2 µm white Isopore polycarbonate filter (EMD Millipore) and stained with
247 DAPI (Life Technologies, catalog S33025) for 5 minutes (600 nM final concentration).
248 The remaining 3 mL was filtered onto the polycarbonate filter. The filter was transferred
249 to a gelatin-coated coverglass that had 1 µL of DI water on it to promote attachment
250 between the filter and the gelatin. After 10 minutes, the filter was removed and the
251 coverglass was sealed to a glass slide containing 10 µL DI water (50).

252

253 *TIRF microscopy*. A lab-built laser microscopy system was used for TIRF, similar to the
254 setup first described by Axelrod (43, 51). Briefly, images were acquired using a Zeiss
255 Observer.A1 microscope with a 100×/1.46 NA oil immersion lens, with an additional 2×
256 magnification after the tube lens. Laser light from 405 nm, 488 nm, 561 nm, and 641 nm
257 sources (Coherent Cube (405 nm and 641 nm) and Coherent Sapphire (488 nm and 561
258 nm) Lasers) was expanded to approximately 1″ diameter, and focused onto the back
259 aperture of the objective using a 500 mm achromatic doublet lens. The laser beams were
260 modulated using a computer-controlled acousto-optic modulator (model number
261 AOTFnC-400.650, AA Opto-Electronic, Osray, France). Frames were acquired every 30
262 ms with a Peltier cooled (-75 ^{o}C) Andor iXON DU897 eMCCD (Fig. 4, 5 SI-1, and SI-2)
263 or Princeton Instruments Excelon ProEM512 CCD (Fig. 6) camera using the software
264 provided by the manufacturer with electron multiplier gain set to 300. The eMCCDs have
265 similar sensitivity and pixel size and the camera change did not affect detection capability.
266 The laser intensity settings on the main laser module were 2.7 mW for 405 nm, 30 mW
267 for 488 nm, 50 mW for 561 nm, and 75 mW for 641 nm.

268

269 *Image processing.* Images were processed using ImageJ version 1.47 (National Institutes
270 of Health). Andor .sif files were read into ImageJ using the Read_SIF plug-in. Twenty-
271 five sequential frames were summed to reduce random background noise. The minimum
272 fluorescence level was normalized for all images acquired with the same laser. The
273 average photon count over the entire view area was measured, and statistical significance
274 assessed using a t-test. For the line profiles, a line was drawn across the mid-point of

three individual bacteria, and the fluorescence intensity along that line was plotted as a function of distance. For the false-colored images, each laser (488 nm and 561 nm) was assigned a color, and images were merged.

Results

Induction of carotenoid biosynthesis

In previous work, a fosmid clone from the Hawaii Ocean Time Series (HOTS), HF10_19P19, was shown to encode retinal biosynthesis and a proteorhodopsin (20). In that study, the expression of these genes could be increased by increasing the copy number of the fosmid in *E. coli*, but could not be controlled directly. Here, we cloned the genes for lycopene, β-carotene, and retinal biosynthesis (Fig. 1) into an expression vector downstream of the *araBAD* promoter, so that the production of carotenoids in *E. coli* can be induced with addition of arabinose or inhibited with addition of glucose to the growth medium. In the presence of glucose, no lycopene, β-carotene, or retinal synthesis was observed (Fig. 2, dotted lines). In the presence of arabinose, *E. coli* harboring plasmid pLY02 synthesized lycopene (Fig. 2A, solid line), *E. coli* harboring plasmid pBC01 synthesized β-carotene (Fig. 2B, solid line), and *E. coli* harboring plasmid pRET04 synthesized retinal (Fig. 2C, solid line). The intermediate phytoene (not shown) was observed in all samples, and some β-carotene accumulated in the retinal-producing strain.

Actinorhodopsin expression

297 The actinorhodopsin gene (*actR*) from *Rhodoluna lacicola* strain MWH-Ta8 (15, 16) was
298 cloned into pMCL200 and expressed in retinal-producing *E. coli* (cells harboring plasmid
299 pRET04). The retinal-producing cells are pale yellow, but turned pink upon induction of
300 actinorhodopsin expression, (Fig. 3A), indicating that actinorhodopsin had folded
301 correctly and incorporated the retinal cofactor (12). ActR was purified in *E. coli*
302 membranes and is visible as a dark band with apparent molecular weight of ~22 kDa in
303 denaturing gel electrophoresis (Fig. 3B). The absorption spectrum of the pink membrane
304 fraction has a clear peak at 528 nm (Fig. 3C), which is in the typical range for microbial
305 rhodopsins when retinal is bound.
306
307 **Visualization of actinorhodopsin using TIRF microscopy**
308 *E. coli* expressing lycopene, β-carotene, retinal, retinal/actinorhodopsin, or
309 actinorhodopsin alone were imaged by TIRF microscopy (Fig. 4 and Fig. SI-1). Lasers
310 with excitation wavelengths of 488 nm and 561 nm were utilized to view the cells. The
311 488 nm laser enabled visualization of the pigment-expressing cells (Fig. 4, left column
312 and Fig. SI-1, left column); however, light of this wavelength scattered through the
313 gelatin, causing a streaking phenomenon. The 561 nm laser selectively excited the
314 retinal/actinorhodopsin-expressing cells. The fluorescence emitted by these cells shows
315 the actinorhodopsin with its bound retinal cofactor is the chromophore (Fig. 4F), as cells
316 expressing retinal alone (Fig. 4D) or actinorhodopsin alone (Fig. SI-1F) are not excited
317 when illuminated with this laser. In addition, cells expressing the precursors to retinal,
318 lycopene (Fig. SI-1D) and β-carotene (Fig. 4B), are also not excited at this wavelength.
319 The average fluorescence intensity measured for each sample as a function of view area

size is summarized in Fig. 4G. The fluorescence observed from retinal/actinorhodopsin-expressing cells excited with the 561 nm laser is significantly more than any other sample type ($p<0.002$). A fluorescence intensity profile across the mid-point of a cell indicates the fluorescence is highest in the membrane in the actinorhodopsin-expressing cells illuminated with the 561 nm laser (Fig. 4H).

TIRF microscopy has potential uses in identification of rhodopsin-expressing cells from environmental samples. However, environmental collections are mixed populations of cells, rather than pure cultures. To demonstrate that cells with and without rhodopsins in a mixed sample can be differentiated, equal volumes of cells expressing β-carotene and retinal/actinorhodopsin were mixed, then excited sequentially with the 561 nm and 488 nm lasers. The fluorescence emitted from cells excited with the 488 nm laser is false-colored cyan, while the fluorescence from cells exposed to the 561 nm laser is colored red, and the images from both lasers are merged. Fig. SI-2 shows the images before the merge, clearly indicating the presence of discrete cell populations in the mixed culture. A pure culture of β-carotene expressing cells is mostly cyan (Fig. 5A), while a pure culture of retinal/actinorhodopsin-expressing cells is mostly red (Fig. 5B). A mixed culture (Fig. 5C) clearly shows two populations of cells, which can be differentiated using TIRF microscopy.

Detection of rhodopsin-containing cells in environmental samples

To demonstrate that TIRF microscopy can detect rhodopsin-containing cells in natural samples, water was collected from the Delaware River and screened by PCR for the

Applied and Environmental Microbiology

presence of rhodopsin-containing microorganisms. Rhodopsin genes were amplified using the degenerate primers SARPR_125F and SARPR_203R (28), and sequencing of the PCR products identified these rhodopsins as related to the rhodopsin found in the SAR11 clade (Fig. SI-3).

Water samples were fixed, stained with DAPI, and concentrated onto polycarbonate filters. Cells were then transferred to gelatin-coated coverslips for imaging. Samples were excited using all four lasers sequentially on the same view area: 405 nm to detect DAPI, 488 nm to visualize carotenoid pigments, 561 nm to find potential rhodopsins, and 641 nm to image Chl-containing organisms (Fig. 6). A number of microorganisms exhibited fluorescence when excited with the 561 nm laser. Some fluoresced when excited with 641 nm (single arrowhead), indicating the presence of Chl in these cells (Fig. 6D), but others were selectively excited with the 561 nm laser (double arrowhead) (Fig. 6C). These are rhodopsin-containing cells.

Discussion

TIRF microscopy

One of the primary challenges to detection of rhodopsins in natural samples has been the very low fluorescent yield of these pigment-protein complexes (40–42). As we demonstrate here, TIRF microscopy is capable of differentiating between unpigmented *E. coli*, *E. coli* producing weakly fluorescent, strongly absorbing carotenoid pigments, and *E. coli* producing weakly fluorescent, strongly absorbing rhodopsin proteins. In addition, in

Applied and Environmental Microbiology

366 the relatively large *E. coli* cells, we can visualize the spatial localization of these
367 pigments or proteins (Fig. 4F, H). The heterologously expressed actinorhodopsin is found
368 in the *E. coli* membrane, as observed both in the membrane preparation (Fig. 3B) and in
369 the fluorescence profiles of the cells (Fig. 4H).
370
371 Because of its sensitivity and low background fluorescence, TIRF microscopy has a
372 variety of uses in the analysis of microbial rhodopsins. It has been used to characterize
373 the mobility of the vertebrate photoreceptor rhodopsin within the cell membrane (52) and
374 subcellular localization of other bacterial proteins (53). Photocycle dynamics of both
375 sensory and ion-pumping rhodopsins over very small temporal and spatial scales have
376 been observed with TIRF microscopy using photochromic fluorescence resonant energy
377 transfer (pcFRET; (54)). Another high resolution technique, confocal laser scanning
378 microscopy (CLSM), also has the potential to detect fluorescence from rhodopsins if
379 outfitted with a photomultiplier. CLSM can provide similar resolution and can be used on
380 either fixed or live cells. However, TIRF microscopy is more powerful for imaging
381 molecules located at or near the membrane (within 100-200 nm of the coverslip), and
382 thus may be more useful for membrane-bound proteins such as rhodopsins. For a
383 comparison of TIRF microscopy, CLSM, and other super-resolution techniques, see the
384 recent review by Schermelleh *et al*. (55). In addition, the source of noise in single-
385 molecule or single-cell imaging arises from Raman and Rayleigh scattering of the liquid
386 (56). TIRF microscopy typically yields higher signal-to-noise ratios compared to CLSM
387 because the imaging volume is much smaller and less background scattering is present.
388 For example, the depth of a typical 40 μm × 40 μm image is around 100 nm for TIRF

389 microscopy, compared to 1 µm for CLSM; therefore, the volume imaged by TIRF is 10-
390 fold smaller than that of CLSM.
391
392 We demonstrate here that in addition to enabling analyses on the single-molecule and
393 single-cell scale, TIRF microscopy can contribute to in situ analyses by differentiating
394 between unpigmented, carotenoid-producing, Chl-producing and rhodopsin-producing
395 microbes in environmental samples. TIRF microscopy is able to identify (B)Chl
396 fluorescence as different from rhodopsin or carotenoid fluorescence. Chl *a* fluorescence
397 emission is closer to 670 nm, while BChl *a* fluorescence emission is in the near-IR
398 (~780-820 nm). In our system, (B)Chl-containing organisms fluoresce when excited with
399 both the 561 nm and 641 nm lasers, while rhodopsin-containing organisms are selectively
400 excited with the 561 nm laser.
401
402 *Actinorhodopsin expression*
403 Actinorhodopsins (ActR) were identified first in a global analysis of metagenomic data
404 (14) and subsequently in some cultivated freshwater Actinobacteria (15). They are
405 predicted to be proton-pumping rhodopsins (15, 38). ActR distribution in Actinobacteria
406 from freshwater environments suggests that they allow Actinobacteria to utilize one of
407 the only resources universally available in those environments – sunlight – to supplement
408 the cellular energy budget. Although their function is currently unconfirmed, we report
409 here the expression of *actR* in a heterologous host. Expression of *actR* in a retinal-
410 producing strain of *E. coli* results in *E. coli* with pink membranes, indicating a rhodopsin
411 with bound retinal. Purification of ActR from the *E. coli* membrane and subsequent

spectroscopy demonstrates that the retinal-bound form of actinorhodopsin has an absorption peak at 528 nm (Fig. 3), similar to the green-light-tuned forms of proteorhodopsin (57).

Production of carotenoid intermediates

The plasmids described here encode the synthesis of lycopene, β-carotene, and retinal, under the control of the arabinose-inducible *araBAD* promoter (Fig. 1). This controllable expression construct allows the plasmids to be propagated without production of carotenoids, which tend to have a deleterious effect on the growth of *E. coli*. The co-production of retinal and actinorhodopsin is clearly an effective way of supplying the actinorhodopsin with a cofactor; no additional proteins are necessary for insertion of the cofactor into actinorhodopsin, as evidenced by the color development (Fig. 3A). These plasmids were used here for proof-of-concept experiments demonstrating that TIRF microscopy can differentiate between unpigmented, carotenoid-producing, and rhodopsin-producing cells (Fig. 4 and 5).

Implications for rhodopsins in environmental samples

Although rhodopsins are widespread among planktonic microbes, carotenoid pigments are even more common (25, 58–60). Even though the absorption spectrum of rhodopsin is red-shifted relative to that of most carotenoids, the similarity in absorption spectra and fluorescent yield makes them difficult to differentiate in bulk samples using traditional methods. However, it is important to distinguish these two populations: bacteria with

rhodopsins are able to utilize light, while carotenoids in the absence of a protein photosystem more likely protect the organism from light-induced damage (61, 62).

Whether a cell has a sensory rhodopsin or an ion-pumping rhodopsin, the rhodopsin mediates the ability to sense and use sunlight. The estimates of rhodopsin abundance based on metagenomic data indicate that an abundance of microbes in illuminated environments utilize sunlight. The discovery in 2001 that a large percentage of microbes in marine surface waters were aerobic anoxygenic phototrophs (AAPs) revolutionized our understanding of the contribution of sunlight to the biological oxidation of organic matter (2, 23). Current estimates indicate that rhodopsin-containing organisms are even more widespread than AAPs (3), and thus that sunlight may play an unexpectedly large role in organic carbon consumption. The TIRF microscopy method described here provides a way to directly identify rhodopsin-expressing cells, even in mixed cultures, and to detect rhodopsin-containing microorganisms in natural samples.

Acknowledgements

The authors gratefully acknowledge Rovshan Mahmudov and Michael Davidson for technical assistance, the University of Delaware Sequencing and Genotyping Facility for sequence data, the Delaware Biotechnology Institute's Bioimaging Center for access to the TIRF microscope, and Bryan Ferlez (Penn State), Thomas Hanson, Clara Chan, and Holly Michael for useful discussions. Research reported in this publication was supported by an Institutional Development Award (IDeA) from the National Institute of General

Applied and Environmental Microbiology

Medical Sciences of the National Institutes of Health under grant number 5 P30 GM103519.

Table and Figure Legends

Table 1. Primers used for cloning carotenoid and actinorhodopsin expression constructs and detection of rhodopsins in Delaware River water. To construct plasmids encoding lycopene, β-carotene, and retinal biosynthesis, primers were designed to amplify specific regions of fosmid clone HF10_19P19 (NCBI accession no. EF100190 (20)). An XbaI site was introduced into primers 19P19_R2 and 19P19_F3, which are reverse complements of each other, so that the *blh* gene could be inserted into plasmid pBC01 (see Fig. 1). To construct an actinorhodopsin expression plasmid, primers F-apa-ta8 and R-ta8-bam were designed to amplify the *actR* gene from *Rhodoluna lacicola* strain MWH-Ta8 (15, 16). Several sets of primers were utilized to screen the genomic DNA from the Delaware River for the presence of actinorhodopsin or proteorhodopsin containing organisms (see Table SI-1). Only the SARPR primers listed in this table successfully amplified rhodopsin genes (28).

Figures:

Figure 1. Carotenoid expression constructs. All genes were PCR-amplified from fosmid HF10_19P19 (20). Plasmid pLY02 encodes lycopene biosynthesis; plasmid pBC01 encodes β-carotene biosynthesis, and pRET04 encodes retinal biosynthesis. Plasmids pLY02 and pBC01 were constructed by amplification of the regions of interest

using primer pairs F1/R1 and F1/R2 (Table 1), respectively, and direct ligation of the product into vector pBAD-TOPO. Plasmid pRET04 was constructed by amplification of the *blh* gene using primer pair F3/R3 and insertion of this product into the XbaI site of pBC01 (see Methods for more detail).

Figure 2. Products of carotenoid-producing *E. coli* strains. Pigments were extracted from *E. coli* grown with glucose, which represses expression due to the *araC* gene product (dotted lines), or arabinose, which induces expression from the *araBAD* promoter (solid lines). **A**. HPLC chromatogram of pigments extracted from *E. coli* harboring plasmid pLY02, monitored at 471 nm. These cells synthesize a single compound with absorption peaks at 471 and 502 nm, characteristic of lycopene (right panel). **B**. HPLC chromatogram of pigments extracted from *E. coli* harboring plasmid pBC01, monitored at 452 nm. This strain produces a compound with absorption peaks at 452 and 478 nm, characteristic of β-carotene (right panel). **C**. HPLC chromatogram of pigments extracted from *E. coli* harboring pRET04, monitored at 380 nm. The major pigment produced by these cells has absorption peaks at 380 nm, typical of retinal (right panel). Some β-carotene is also present in this strain (not shown).

Figure 3. Expression of actinorhodopsin in *E. coli*. The *actR* gene was cloned into plasmid pMCL200 to produce plasmid pTAR, and co-transformed into the epi300 strain along with plasmid pRET04. **A**. Concentrated cell solution of *E. coli* epi300 with plasmids pRET04 and pTAR (left) and pRET04 and pMCL200 (right). The pink color indicates that the actinorhodopsin has incorporated the retinal cofactor. **B**. SDS-PAGE of

Applied and Environmental Microbiology

partially purified membrane preparations from *E. coli* with plasmids pRET04 and pTAR (1), partially purified membrane preparations from *E. coli* with plasmids pRET04 and pMCL200 (2), and protein standard (3). The band corresponding to ActR at ~22 kDa is labeled. **C**. Absorption spectrum of partially purified membranes from *E. coli* with plasmids pRET04 and pTAR.

Figure 4. TIRF microscopy of engineered *E. coli* strains. Cells were affixed to a gelatin coated chambered glass coverslip and viewed after being illuminated with a 488 nm laser (left column) or a 561 nm laser (right column). The 488 nm laser excites both carotenoids and rhodopsins, but the 561 nm laser excites rhodopsins exclusively. **A. and B**. *E. coli* + pBC01 (β-carotene-expressing). **C. and D.** *E. coli* + pRET04/pMCL200 (retinal-expressing). **E. and F.** *E. coli* + pRET04/pTAR (retinal- and actinorhodopsin-expressing). **G**. Fluorescence intensity observed for each 20 μm^2 view area when excited with the 488 nm or 561 nm laser. The asterisk indicates fluorescence emitted from actinorhodopsin-expressing cells is significantly more than any other cell type ($p<0.002$). **H.** Fluorescence intensity line profile across three individual actinorhodopsin-expressing cells excited with 561 nm laser showing fluorescence localized to membranes. An example line profile is indicated by an arrow in panel F.

Figure 5. TIRF microscopy of pure cultures and mixed β-carotene- and actinorhodopsin-expressing *E. coli*. A glass coverslip was coated with 0.5% gelatin, and cells were allowed to attach for 10 minutes. Unattached cells were washed away and the chamber was flooded with media before imaging. The same field of view was excited

525 with the 488 nm laser and the 561 nm laser. Fluorescence observed from the 488 nm laser
526 was colored cyan, while fluorescence from the 561 nm laser was colored red, and the
527 images were merged. **A**. A pure culture of *E. coli* with plasmid pBC01 (β-carotene-
528 expressing cells) was imaged with both lasers sequentially. Most of the cells appear cyan
529 because they were only excited with the 488 nm laser. **B**. A pure culture of *E. coli* with
530 plasmids pRET04 and pTAR (actinorhodopsin-expressing cells) was imaged with both
531 lasers, and appears red due to the fluorescence from the 561 nm laser excitation. **C**. A
532 mixed culture of β-carotene- and actinorhodopsin-expressing cells was imaged with both
533 488 nm and 561 nm lasers. Both populations of cells can be clearly viewed, as the β-
534 carotene-expressing cells respond only to the 488 nm laser, and thus are cyan, while the
535 actinorhodopsin-expressing cells are illuminated by the 561 nm laser, and are colored red.
536
537 **Figure 6. TIRF microscopy of natural water samples.** Water samples were fixed,
538 stained with DAPI, and filtered onto a 0.2 µm polycarbonate filter before being
539 transferred to a gelatin-coated glass coverslip. Samples were viewed after being
540 illuminated with a 405 nm laser (**A**), a 488 nm laser (**B**), a 561 nm laser (**C**), or a 641 nm
541 laser (**D**). The 405 nm laser excites the DAPI stain, indicating the presence of DNA-
542 containing cells. The 641 nm laser illuminates (bacterio)chlorophyll-containing cells
543 (labeled with a single arrowhead). Cells that fluoresce only when excited with the 561 nm
544 laser (labeled with a double arrowhead) are rhodopsin-containing cells. Each panel shows
545 the same view of a single representative sample, and the scale bar is 1 µm.
546
547 **References**

1. **Geider RJ, Delucia EH, Falkowski PG, Finzi AC, Grime JP, Grace J, Kana TM, La Roche J, Long SP, Osborne BA, Platt T, Prentice IC, Raven JA, Schlesinger WH, Smetacek V, Stuart V, Sathyendranath S, Thomas RB, Vogelmann TC, Williams P, Woodward FI**. 2001. Primary productivity of planet earth: biological determinants and physical constraints in terrestrial and aquatic habitats. Glob. Chang. Biol. **7**:849–882.

2. **Moran MA, Miller WL**. 2007. Resourceful heterotrophs make the most of light in the coastal ocean. Nat. Rev. Microbiol. **5**:792–800.

3. **Kirchman DL, Hanson TE**. 2013. Bioenergetics of photoheterotrophic bacteria in the oceans. Environ. Microbiol. Rep. **5**:188–199.

4. **Hoff WD, Jung K-H, Spudich JL**. 1997. Molecular mechanism of photosignaling by archaeal sensory rhodopsins. Annu. Rev. Biophys. Biomol. Struct. **26**:223–258.

5. **Sharma AK, Spudich JL, Doolittle WF**. 2006. Microbial rhodopsins: functional versatility and genetic mobility. Trends Microbiol. **14**:463–469.

6. **Lanyi JK, Balashov SP**. 2008. Xanthorhodopsin: a bacteriorhodopsin-like proton pump with a carotenoid antenna. Biochim. Biophys. Acta **1777**:684–688.

7. **Spudich JL, Yang CS, Jung KH, Spudich EN**. 2000. Retinylidene proteins: structures and functions from archaea to humans. Annu. Rev. Cell Dev. Biol. **16**:365–392.

8. **Irieda H, Morita T, Maki K, Homma M, Aiba H, Sudo Y**. 2012. Photo-induced regulation of the chromatic adaptive gene expression by Anabaena Sensory Rhodopsin. J. Biol. Chem. **287**:32485–32493.

9. **Schobert B, Lanyi JK**. 1982. Halorhodopsin is a light-driven chloride pump. J. Biol. Chem. **257**:10306–10313.

10. **Inoue K, Ono H, Abe-Yoshizumi R, Yoshizawa S, Ito H, Kogure K, Kandori H**. 2013. A light-driven sodium ion pump in marine bacteria **4**:1678.

11. **Yoshizawa S, Kumagai Y, Kim H, Ogura Y, Hayashi T, Iwasaki W, DeLong EF, Kogure K**. 2014. Functional characterization of flavobacteria rhodopsins reveals a unique class of light-driven chloride pump in bacteria. Proc. Natl. Acad. Sci. **111**:6732–6737.

12. **Beja O, Aravind L, Koonin E V, Suzuki MT, Hadd A, Nguyen LP, Jovanovich SB, Gates CM, Feldman RA, Spudich JL, Spudich EN, Delong EF**. 2000. Bacterial rhodopsin: evidence for a new type of phototrophy in the sea. Science **289**:1902–1906.

13. **Oesterhelt D, Stockenius W**. 1971. Rhodopsin-like protein from the purple membrane of *Halobacterium halobium*. Nature **233**:149–152.

14. **Sharma AK, Zhaxybayeva O, Papke RT, Doolittle WF**. 2008. Actinorhodopsins: proteorhodopsin-like gene sequences found predominantly in non-marine environments. Environ. Microbiol. **10**:1039–1056.

15. **Sharma AK, Sommerfeld K, Bullerjahn GS, Matteson AR, Wilhelm SW, Jezbera J, Brandt U, Doolittle WF, Hahn MW**. 2009. Actinorhodopsin genes discovered in diverse freshwater habitats and among cultivated freshwater Actinobacteria. ISME J. **3**:726–737.

16. **Hahn M, Schmidt J, Taipale SJ, Doolittle WF, Koll U**. 2014. *Rhodoluna lacicola* gen. nov., sp. nov., a planktonic freshwater bacterium with stream-lined genome. Int. J. Syst. Evol. Microbiol.

17. **Gómez-Consarnau L, Akram N, Lindell K, Pedersen A, Neutze R, Milton DL, González JM, Pinhassi J**. 2010. Proteorhodopsin phototrophy promotes survival ofmMarine bacteria during starvation. PLoS Biol **8**:e1000358.

18. **Gómez-Consarnau L, González JM, Coll-Lladó M, Gourdon P, Pascher T, Neutze R, Pedrós-Alió C, Pinhassi J**. 2007. Light stimulates growth of proteorhodopsin-containing marine Flavobacteria. Nature **445**:210–213.

19. **DeLong EF, Béjà O**. 2010. The light-driven proton pump proteorhodopsin enhances bacterial survival during tough times. PLoS Biol. **8**:e1000359.

20. **Martinez A, Bradley AS, Waldbauer JR, Summons RE, Delong EF**. 2007. Proteorhodopsin photosystem gene expression enables photophosphorylation in a heterologous host. Proc. Natl. Acad. Sci. **104**:5590–5595.

21. **Li WKW, Wood AM**. 1988. Vertical distribution of North Atlantic ultraphytoplankton: analysis by flow cytometry and epifluorescence microscopy. Deep Sea Res. Part A. Oceanogr. Res. Pap. **35**:1615–1638.

22. **Olson RJ, Zettler ER, Anderson OK**. 1989. Discrimination of eukaryotic phytoplankton cell types from light scatter and autofluorescence properties measured by flow cytometry. Cytometry **10**:636–643.

23. **Kolber ZS, Van Dover CL, Niederman RA, Falkowski PG**. 2000. Bacterial photosynthesis in surface waters of the open ocean. Nature **407**:177–179.

24. **Rusch DB, Halpern AL, Sutton G, Heidelberg KB, Williamson S, Yooseph S, Wu D, Eisen JA, Hoffman JM, Remington K, Beeson K, Tran B, Smith H, Baden-Tillson H, Stewart C, Thorpe J, Freeman J, Andrews-Pfannkoch C, Venter JE, Li K, Kravitz S, Heidelberg JF, Utterback T, Rogers Y-H, Falcón**

LI, Souza V, Bonilla-Rosso G, Eguiarte LE, Karl DM, Sathyendranath S, Platt T, Bermingham E, Gallardo V, Tamayo-Castillo G, Ferrari MR, Strausberg RL, Nealson K, Friedman R, Frazier M, Venter JC. 2007. The Sorcerer II Global Ocean Sampling expedition: Northwest Atlantic through Eastern Tropical Pacific. PLoS Biol. **5**:e77.

25. **McCarren J, DeLong EF**. 2007. Proteorhodopsin photosystem gene clusters exhibit co-evolutionary trends and shared ancestry among diverse marine microbial phyla. Environ. Microbiol. **9**:846–858.

26. **Atamna-Ismaeel N, Sabehi G, Sharon I, Witzel KP, Labrenz M, Jurgens K, Barkay T, Stomp M, Huisman J, Beja O**. 2008. Widespread distribution of proteorhodopsins in freshwater and brackish ecosystems. ISME J. **2**:656–662.

27. **Campbell BJ, Waidner LA, Cottrell MT, Kirchman DL**. 2008. Abundant proteorhodopsin genes in the North Atlantic Ocean. Environ. Microbiol. **10**:99–109.

28. **Lami R, Cottrell MT, Campbell BJ, Kirchman DL**. 2009. Light-dependent growth and proteorhodopsin expression by Flavobacteria and SAR11 in experiments with Delaware coastal waters. Environ. Microbiol. **11**:3201–9.

29. **Hahn MW**. 2009. Description of seven candidate species affiliated with the phylum Actinobacteria, representing planktonic freshwater bacteria. Int. J. Syst. Evol. Microbiol. **59**:112–117.

30. **Zhao M, Chen F, Jiao N**. 2009. Genetic diversity and abundance of Flavobacterial proteorhodopsin in China Seas. Appl. Environ. Microbiol. **75**:529–533.

31. **Yoshizawa S, Kawanabe A, Ito H, Kandori H, Kogure K**. 2012. Diversity and functional analysis of proteorhodopsin in marine Flavobacteria. Environ. Microbiol. **14**:1240–1248.

32. **Allen LZ, Allen EE, Badger JH, McCrow JP, Paulsen IT**. 2012. Influence of nutrients and currents on the genomic composition of microbes across an upwelling mosaic. ISME J. **6**:1403–1414.

33. **Yin Q, Fu B, Li B, Shi X, Inagaki F, Zhang X-H**. 2013. Spatial variations in microbial community composition in surface seawater from the ultra-oligotrophic center to rim of the South Pacific Gyre. PLoS One **8**:e55148.

34. **Béjà O, Suzuki MT**. 2008. Photoheterotrophic marine prokaryotes BT - Microbial ecology of the oceans, p. 131–157. *In* Microbial ecology of the oceans. John Wiley & Sons, Inc.

35. **Martínez-García M, Swan BK, Poulton NJ, Gomez ML, Masland D, Sieracki ME, Stepanauskas R**. 2012. High-throughput single-cell sequencing identifies photoheterotrophs and chemoautotrophs in freshwater bacterioplankton. ISME J. **6**:113–123.

36. **Ugalde JA, Podell S, Narasingarao P, Allen EE**. 2011. Xenorhodopsins, an enigmatic new class of microbial rhodopsins horizontally transferred between archaea and bacteria. Biol. Direct **6**:1–8.

37. **Kwon SK, Kim BK, Song JY, Kwak MJ, Lee CH, Yoon JH, Oh TK, Kim JF**. 2013. Genomic makeup of the marine Flavobacterium *Nonlabens* (*Donghaeana*) *dokdonensis* and identification of a novel class of rhodopsins. Genome Biol. Evol. **5**:187–199.

38. **Brown LS**. 2014. Eubacterial rhodopsins — Unique photosensors and diverse ion pumps. BBA - Bioenerg. **1837**:553–561.

39. **Alexiev U, Farrens DL**. 2013. Fluorescence spectroscopy of rhodopsins: Insights and approaches. BBA - Bioenerg. 1–16.

40. **Cheminal a., Léonard J, Kim SYY, Jung K-HH, Kandori H, Haacke S**. 2013. Steady state emission of the fluorescent intermediate of Anabaena Sensory Rhodopsin as a function of light adaptation conditions. Chem. Phys. Lett. **587**:75–80.

41. **Kochendoerfer GG, Mathies RA**. 1996. Spontaneous emission study of the femtosecond isomerization dynamics of rhodopsin. J. Phys. Chem. **100**:14526–14532.

42. **Kralj JM, Douglass AD, Hochbaum DR, Maclaurin D, Cohen AE**. 2012. Optical recording of action potentials in mammalian neurons using a microbial rhodopsin. Nat. Chem. Biol. **9**:90–95.

43. **Axelrod D**. 2008. Chapter 7 Total internal reflection fluorescence microscopy BT - Biophysical tools for biologists, Volume Two: In vivo techniques, p. 169–221. *In* Dr John J Correia and Dr H William Detrich, III (ed.), Biophysical Tools for Biologists, Volume Two: In Vivo Techniques. Academic Press.

44. **Hahn MW, Stadler P, Wu QL, Pöckl M**. 2004. The filtration–acclimatization method for isolation of an important fraction of the not readily cultivable bacteria. J. Microbiol. Methods **57**:379–390.

45. **Nakano Y, Yoshida Y, Yamashita Y, Koga T**. 1995. Construction of a series of pACYC-derived plasmid vectors. Gene **162**:157–158.

686 46. **Bender GR, Sutton S V, Marquis RE**. 1986. Acid tolerance, proton
687 permeabilities, and membrane ATPases of oral streptococci. Infect. Immun.
688 **53**:331–338.

689 47. **Laemmli UK**. 1970. Cleavage of structural proteins during the assembly of the
690 head of bacteriophage T4. Nature **227**:680–685.

691 48. **Maresca JA, Braff JC, DeLong EF**. 2009. Characterization of canthaxanthin
692 biosynthesis genes from an uncultured marine bacterium. Environ. Microbiol. Rep.
693 **1**:524–534.

694 49. **Doktycz MJ, Sullivan CJ, Hoyt PR, Pelletier DA, Wu S, Allison DP**. 2003.
695 AFM imaging of bacteria in liquid media immobilized on gelatin coated mica
696 surfaces. Ultramicroscopy **97**:209–216.

697 50. **Ouverney CC, Fuhrman JA**. 1999. Combined microautoradiography-16S rRNA
698 probe technique for determination of radioisotope uptake by specific microbial cell
699 types in situ. Appl. Envir. Microbiol. **65**:1746–1752.

700 51. **Axelrod D**. 1981. Cell-substrate contacts illuminated by total internal reflection
701 fluorescence. J. Cell Biol. **89**:141–145.

702 52. **Kim T-Y, Uji-i H, Möller M, Muls B, Hofkens J, Alexiev U**. 2009. Monitoring
703 the interaction of a single G-protein key binding site with rhodopsin disk
704 membranes upon light activation. Biochemistry **48**:3801–3803.

705 53. **Garner EC, Bernard R, Wang W, Zhuang X, Rudner DZ, Mitchison T**. 2011.
706 Coupled, circumferential motions of the cell wall synthesis machinery and MreB
707 filaments in *B. subtilis*. Science **333**:222–225.

708 54. **Bayraktar H, Fields AP, Kralj JM, Spudich JL, Rothschild KJ, Cohen AE**.
709 2012. Ultrasensitive measurements of microbial rhodopsin photocycles using
710 photochromic FRET. Photochem. Photobiol. **88**:90–97.

711 55. **Schermelleh L, Heintzmann R, Leonhardt H**. 2010. A guide to super-resolution
712 fluorescence microscopy. J. Cell Biol. **190**:165–75.

713 56. **Funatsu T, Harada Y, Tokunaga M, Saito K, Yanagida T**. 1995. Imaging of
714 single fluorescent molecules and individual ATP turnovers by single myosin
715 molecules in aqueous solution. Nature **374**:555–9.

716 57. **Man D, Wang W, Sabehi G, Aravind L, Post AF, Massana R, Spudich EN,**
717 **Spudich JL, Beja O**. 2003. Diversification and spectral tuning in marine
718 proteorhodopsins. EMBO J. **22**:1725–1731.

719 58. **Du H, Jiao N, Hu Y, Zeng Y**. 2006. Diversity and distribution of pigmented
720 heterotrophic bacteria in marine environments. FEMS Microbiol. Ecol. **57**:92–105.

721 59. **Asker D, Beppu T, Ueda K**. 2007. Unique diversity of carotenoid-producing
722 bacteria isolated from Misasa, a radioactive site in Japan. Appl. Microbiol.
723 Biotechnol. **77**:383–392.

724 60. **Stafsnes M, Josefsen K, Kildahl-Andersen G, Valla S, Ellingsen T, Bruheim P**.
725 2010. Isolation and characterization of marine pigmented bacteria from Norwegian
726 coastal waters and screening for carotenoids with UVA-blue light absorbing
727 properties. J. Microbiol. **48**:16–23.

728 61. **Tuveson RW, Larson RA, Kagan J**. 1988. Role of cloned carotenoid genes
729 expressed in *Escherichia coli* in protecting against inactivation by near-UV light
730 and specific phototoxic molecules. J. Bacteriol. **170**:4675–4680.

731 62. **Sandmann G, Kuhn S, Böger P**. 1998. Evaluation of structurally different
732 carotenoids in *Escherichia coli* transformants as protectants against UV-B
733 radiation. Appl. Environ. Microbiol. **64**:1972–1974.

734

Applied and Environmental Microbiology

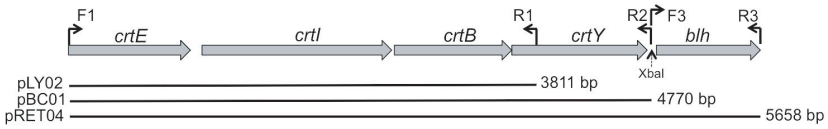

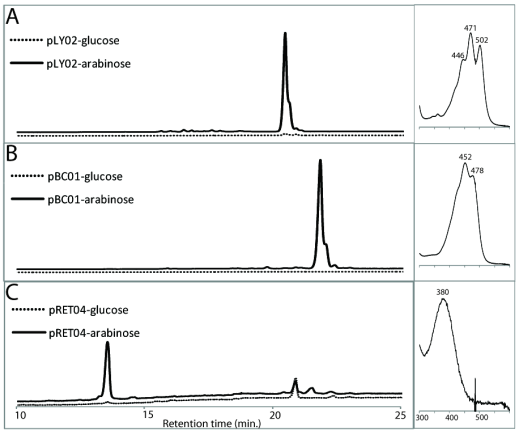

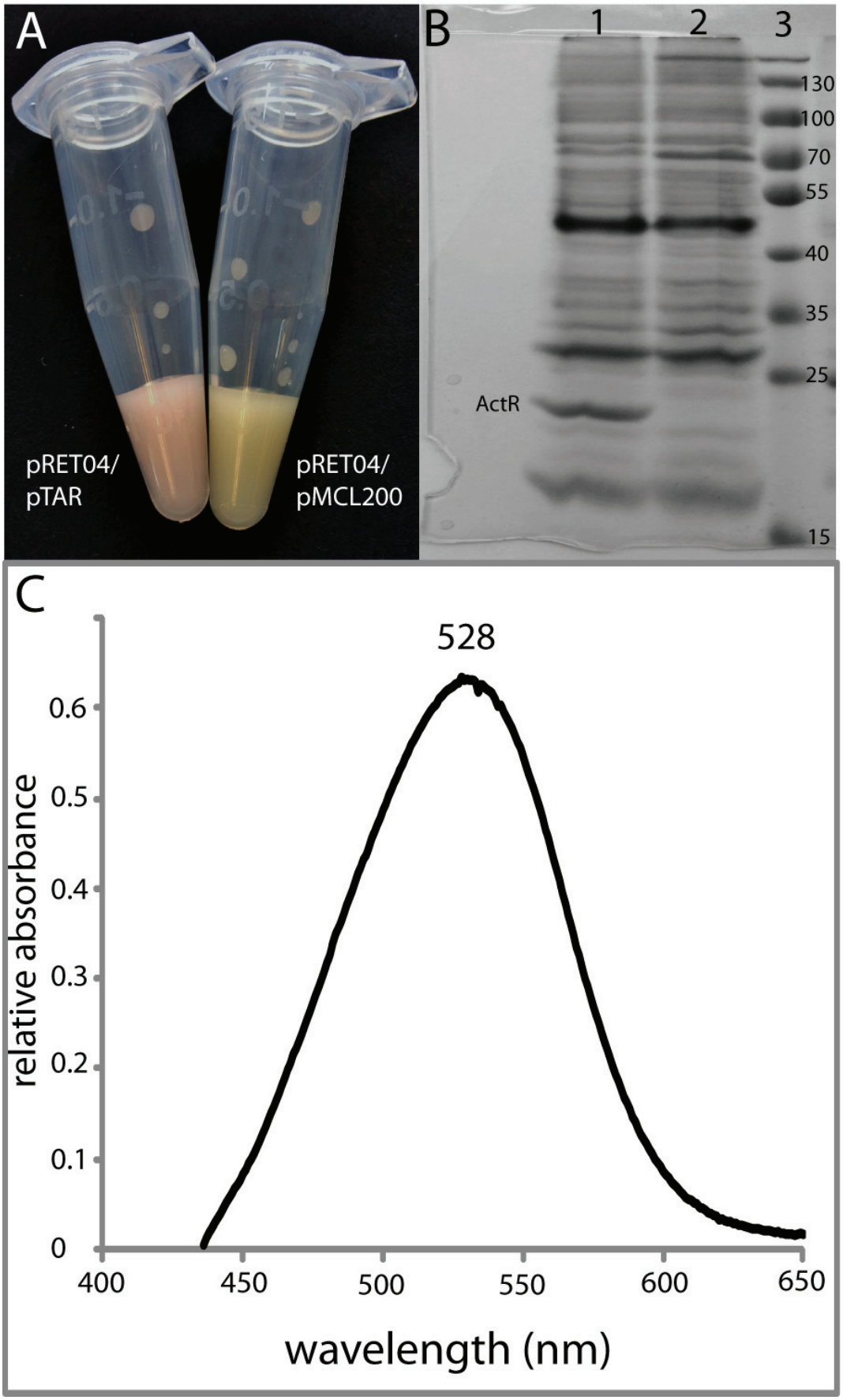

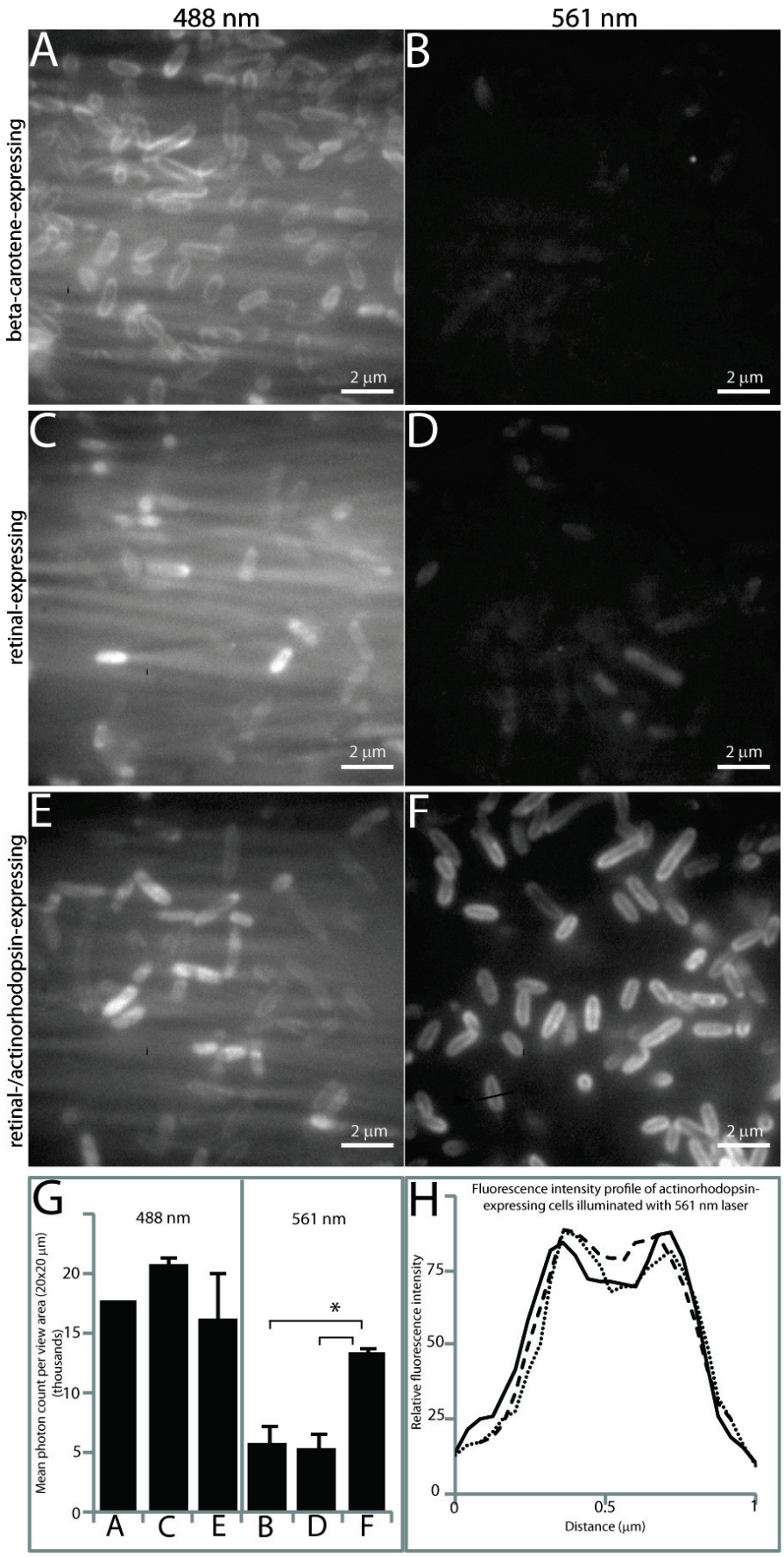

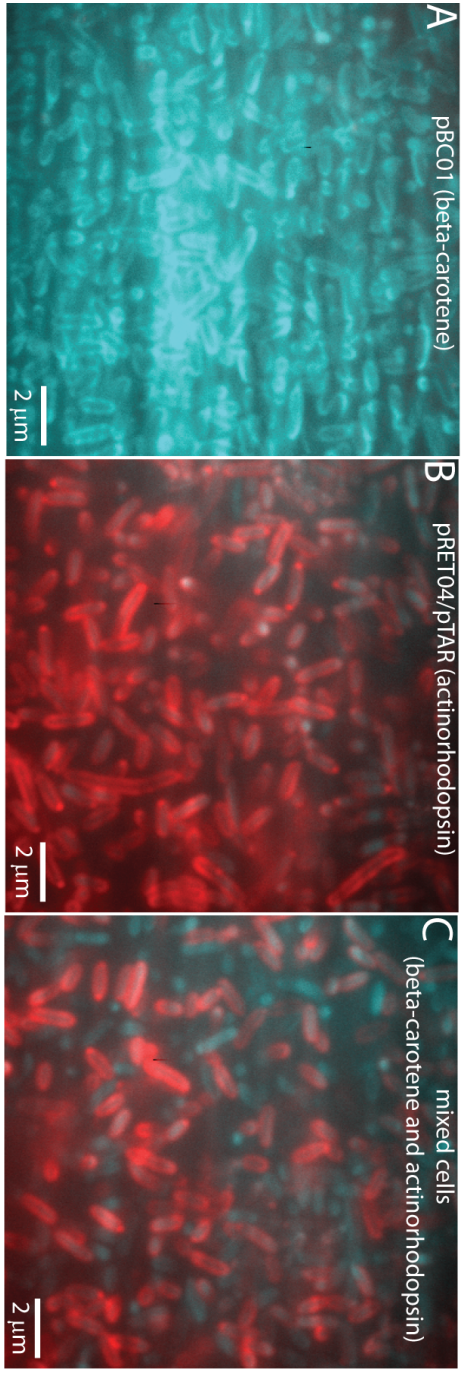
A
pBC01 (beta-carotene)
2 µm
B
pRET04/pTAR (actinorhodopsin)
2 µm
C
mixed cells
(beta-carotene and actinorhodopsin)
2 µm

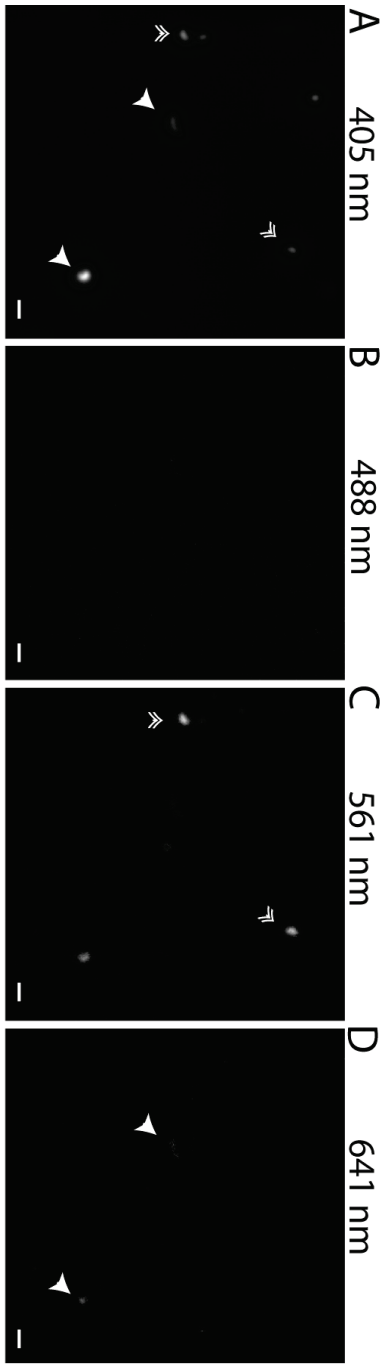
A
405 nm
B
488 nm
C
561 nm
D
641 nm

Primer name	Primer sequence (5' → 3')	Gene(s) in product	Template	Restriction site(s)
19P19_F1	ATG ACA GAG AAC ATA GCC AGC C		Fosmid HF10_19P19	–
19P19_R1	GCG TTG TCT TGA GAG CTC GGT CTG C	*crtE, crtI, crtB, crtY* (partial)	Fosmid HF10_19P19	–
19P19_R2	CG CCG TCT AGA GGC GTT TTG C	*crtE, crtI, crtB, crtY*	Fosmid HF10_19P19	XbaI
19P19_F3	G CAA AAC GCCTCT AGA CGG CG	*blh*	Fosmid HF10_19P19	XbaI
19P19_R3	GCT TGT TCG GGT CAT GGC TGT G		Fosmid HF10_19P19	–
F-apa-ta8	CCC GGG CCC ATG AAC ACA TTG TCT AAT G	*actR*	*Rhodoluna lacicola* genomic DNA	ApaI
R-ta8-bam	CGC GGA TCC TTA GGC GTC TTT GAA C	*actR*	*Rhodoluna lacicola* genomic DNA	BamHI

*